Acta Crystallographica Section B
Structural Science
ISSN 0108-7681

Structure of lithium benzilate hemihydrate solved by simulated annealing and difference Fourier synthesis from powder data

Asiloé J. Mora,[a,b]* Andrew N. Fitch,[b] Belkis M. Ramirez,[a] Gerzon E. Delgado,[a] Michela Brunelli[b] and Jonathan Wright[b]

[a]Laboratorio de Cristalografía, Facultad de Ciencias, Departamento de Química, Universidad de Los Andes, La Hechicera, Mérida 5101, Venezuela, and [b]ESRF, BP220, F-38043 Grenoble CEDEX, France

Correspondence e-mail: simonetta@icnet.com.ve

Received 14 October 2002
Accepted 27 February 2003

The crystal structure of lithium benzilate hemihydrate ($C_{14}H_{11}O_3^-Li^+\cdot 0.5H_2O$) was solved from synchrotron powder diffraction data. This compound crystallizes in the monoclinic space group $P2_1/a$. The structure was solved *via* the direct space search for two benzilate fragments using the simulated-annealing program *DASH*, localization of the lithium ions and water molecule from a difference Fourier map, and a restrained Rietveld refinement (R_{wp} = 0.0687). The structure is a coordination polymer of $[Li_2(C_{14}H_{11}O_3)_2\cdot H_2O]_2$ tetramers building helical fourfold one-dimensional channels parallel to [010]. Inside the channels the tetrahedral coordination spheres of the lithium ions contain hydroxyl and carbonyl groups, and water molecules. The water molecule functions as the cohesive entity forming extended hydrogen-bonded chains running along [010], and bifurcated donor hydrogen bonds with the two nearest carboxylates. At the outer edge of the channels, weaker intermolecular C—H···Ph hydrogen bonds along [100] and [001] contribute to the supramolecular aggregation of the structure.

1. Introduction

The determination of the structure of lithium benzilate hemihydrate was undertaken as part of our study of benzilic acid, and its alkali and metal derivatives. This is an α-glycolic acid that has long been used in the preparation of anti-muscarinic agents (*i.e.* Drescher *et al.*, 1999; Lee *et al.*, 1996; Hiramatsu *et al.*, 1994; Johnston *et al.*, 1985) and has shown X-ray diffuse scattering as a result of packing problems (Mora *et al.*, 2003). In the derivatives the benzilate moiety has two

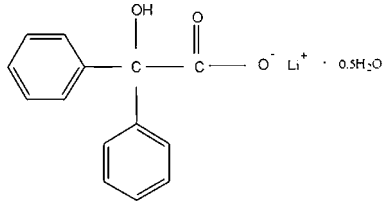

phenyl rings oriented as propeller blades, and hydroxyl and carboxylate groups which have the potential to form hydrogen bonds and interact with the charged field of a counter-ion. Therefore, packing in the solid state should comprise diverse cohesive interactions such as aromatic ($\pi\cdots\pi$, C—H···π, O···H—O) and coordination polymer formation around the alkali or metal ion. In the interest of investigating the chelating and hydrogen-bonding capabilities of the benzilate anion, some metal derivatives of benzilic acid were prepared and characterized by single-crystal X-ray diffraction (Rojas, 2001). Here we report on the structure of another derivative: lithium benzilate hemihydrate, which was obtained as a

polycrystalline powder and was solved by a combination of simulated annealing and difference Fourier maps from X-ray powder diffraction data. This structure, once Rietveld-refined, helps us to solve by the same methodology the complex structure of benzilic acid (Mora *et al.*, 2003).

2. Experimental

2.1. Synthesis and specimen preparation

Lithium benzilate was obtained as a yellow polycrystalline precipitate by the slow evaporation of an aqueous equimolar (20 mmol) solution of benzilic acid (Aldrich, 99+%) and LiOH (Aldrich, 98+%). A small amount of the precipitate was lightly ground with a pestle in an agate mortar and placed into a 1.5 mm diameter borosilicate glass capillary.

2.2. Data collection

The sealed capillary was mounted on the axis of the high-resolution powder diffractometer of beamline BM16 at the European Synchrotron Radiation Facility (ESRF) in Grenoble, France (Fitch, 1995). X-rays with wavelength 0.803030 (1) Å were selected from the white bending-magnet source using the double-crystal Si (111) monochromator. The diffracted beam was analyzed with nine Ge (111) crystal analyzers separated by 2° intervals and detected with nine Na(Tl)I scintillation counters. Diffraction data were collected at room temperature in a continuous scanning mode for several hours while spinning the capillary to improve randomization of the individual crystallites. The data were normalized against the decay of the beam, monitor counts and detector efficiency and converted into step scan data of 0.003° 2θ.

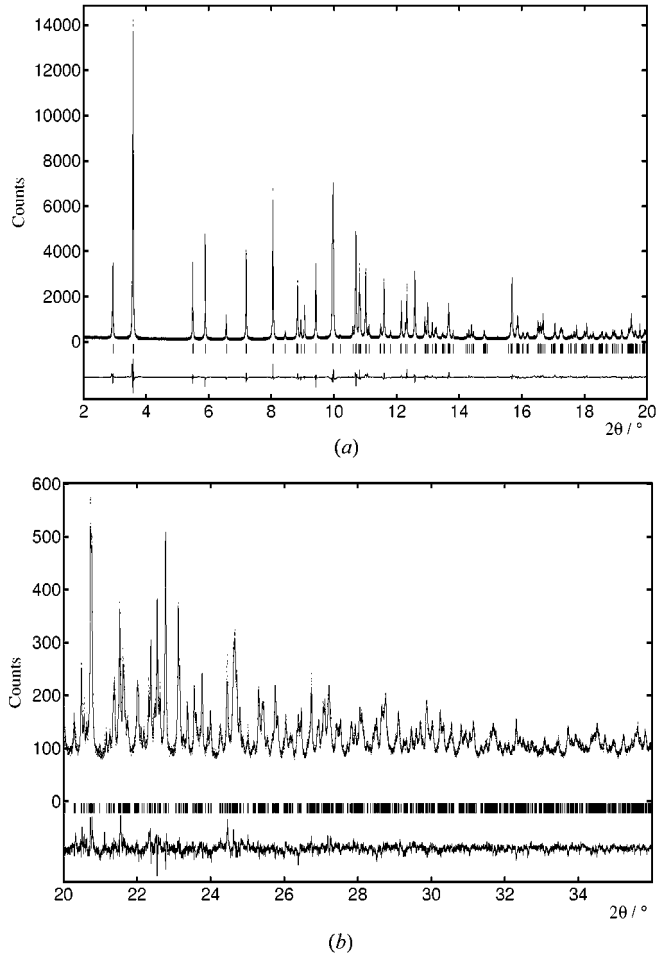

Figure 1
Final observed (points), calculated (lines) and difference profiles for the Rietveld refinement of lithium benzilate hemihydrate: (*a*) low-angle data; (*b*) high-angle data.

Table 1
Experimental details.

Crystal data	
Chemical formula	$C_{28}H_{22}O_6Li_2{\cdot}H_2O$
M_r	486.35
Cell setting, space group	Monoclinic, $P2_1/a$
a, b, c (Å)	34.1916 (2), 5.5346 (1), 14.0289 (1)
β (°)	113.998 (1)
V (Å^3)	2425.31 (5)
Z	8
D_x (Mg m^{-3})	1.332
Radiation type	Synchrotron
μ (mm^{-1})	0.087
Temperature (K)	295
Specimen form, colour	Cylinder (particle morphology: thin powder), yellow
Specimen size (mm)	40 × 1.5 × 1.5
Data collection	
Diffractometer	Beamline BM16, ESRF, France
Data preparation method	Specimen mounting: borosilicate glass capillary; mode: transmission; scan method: continuous
2θ (°)	$2\theta_{min}$ = 1.0, $2\theta_{max}$ = 35.998, increment = 0.003
Refinement	
R factors and goodness-of-fit	R_p = 0.056, R_{wp} = 0.068, R_{exp} = 0.030, S = 2.43
Wavelength of incident radiation (Å)	0.803030 (1)
Excluded region(s)	None
Profile function	Pseudo-Voigt
No. of parameters	221

Computer programs: *GSAS* (Larson & Von Dreele, 1998).

2.3. Indexing

The first 30 peaks of the powder diffraction pattern (see Fig. 1) were fitted using the *DASH* program (David *et al.*, 2001) and their refined positions were input into the auto-indexing program *DICVOL* (Boultif & Louër, 1991). The solution with the highest figures of merit [$M(30)$ = 14.7 (de Wolff, 1968); $F(30)$ = 104.1 (Smith & Snyder, 1979)] indexed all the peaks with a monoclinic cell. Systematic absences indicated the space group $P2_1/a$. Relevant details are summarized in Table 1.

2.4. Structural solution and Rietveld refinement

The structure was solved using the *DASH* program (David *et al.*, 2001). This attempts to minimize the difference between observed and calculated intensities by a simulated-annealing approach that moves molecules (or fragments) within the unit

cell, varying their positions, orientations and, when appropriate, their conformation. For the structural solution, 348 intensities were extracted from the experimental diffraction pattern by carrying out a Pawley (1981) refinement in the angular range $1 \leq 2\theta \leq 23.25^\circ$, as implemented in the program *DASH*. A starting model of the benzilate moiety was assembled using the sketching facilities of *MATERIALS STUDIO* (Molecular Simulations Inc., 2001), assuming that the bulky phenyls which form the hydrophobic portion of the molecule had conformations similar to those seen in other benzilate derivatives (Vyas *et al.*, 1978; Rojas, 2001). Two benzilate ions ($Z' = 2$) were introduced into the cell, which implied that a total of 20 parameters were to be found by the program *DASH* during the minimization process: six coordinates to describe the positions of the two centers of mass, eight quaternions describing their orientations and six torsion angles to describe the conformation about the α carbon atoms. The simulated-annealing routine was run in default mode and after 3068×10^6 moves, requiring approximately 2 h of computer time on a Pentium III 128.0 MB RAM Portable PC, a solution with a χ^2 of 1015 was obtained. The criterion to accept the solution was based more on the soundness of the solution in terms of crystal packing than on the agreement between the calculated and observed patterns, and at this point the relatively high χ^2 value (16 times the value of the Pawley χ^2) was attributed to electron density that remained to be found. During the simulated-annealing minimization the conformation of the benzilate fragments changed slightly (starting values for the torsion angles to describe the orientation of the carboxylate and the two phenyl rings: +30.8, −91.8, −174.7; final values for each independent fragment: +39.0, −100.6, −166.0 and +16.3, −116.0 and −148.1). The solution derived from the simulated-annealing procedure of *DASH* was taken as the starting model of a Rietveld (1969) refinement using the program *GSAS* (Larson & Von Dreele, 1998). The bond distances and angles of the hydroxyl, carboxylate and phenyl groups of both benzilate anions were restrained to reasonable values (Wilson, 1995), weighted by 0.001 Å and 2°, respectively. H atoms were placed in calculated positions and then refined with C—H and O—H distances restrained to be 0.998 Å (weighted 0.001 Å). In addition, C atoms and H atoms in phenyl rings were restrained to be planar, with the deviation from planarity set to be less than 0.01 Å. The background was described by the automatic linear extrapolation of 24 points throughout the whole pattern. The peak shapes were modeled using a pseudo-Voigt function that included an axial divergence asymmetry correction (van Laar & Yelon, 1984; Finger *et al.*, 1994). An overall isotropic temperature factor was refined. The refinement of the partial structure was promising, yielding values of $R_{wp} = 0.21$ and $\chi^2 = 51.8$. A very clean difference Fourier map was then calculated, in which three peaks clearly stood out. The first peak was at least twice as strong as the other two and it was assigned to the oxygen of a water molecule co-crystallized during the synthesis. The other remaining peaks were assigned as the lithium ions. These atoms were added to the model and Rietveld refined with the H atoms of the water molecule placed in calculated positions and their geometry restrained, as in the other H atoms in the structure. It was not necessary to add any constraint regarding the coordination geometry around the lithium ions. Individual isotropic temperature factors were refined for the water molecule and lithium ions. The refinement of 221 variables was robust and convergence was quickly achieved yielding $R_{wp} = 0.068$ and $\chi^2 = 5.89$. Agreement between the observed and calculated pattern is excellent (Fig. 1). An impurity present in trace quantities can be spotted in the background (*i.e.* peaks at 15.22 and 16.40° 2θ) and contributes to the value of χ^2. The largest residual in the final difference Fourier map is +0.26 e Å^{-3}, and it is located 0.76 Å from the oxygen of the water molecule. The presence of such small residuals can be attributed to either insufficient modeling of the thermal vibration of the water molecule or orientational disorder of the water molecule with H atoms partially placed in three rather than two positions. The positional parameters and isotropic temperature factors have been deposited.[1] The Rietveld plot, powder diffraction data and the refined structural parameters have been deposited.

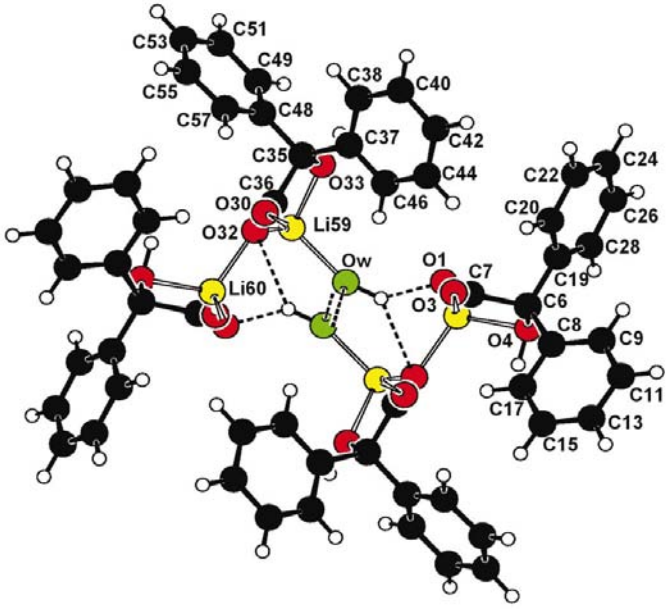

Figure 2
The $[Li_2(C_{14}H_{11}O_3)_2 \cdot H_2O]_2$ tetramers that build the fourfold helical-dimensional channels parallel to [010]. The numbering scheme of the atoms is also shown.

3. Results and discussion

3.1. Molecular structure

The structure of lithium benzilate is depicted in Fig. 2. Each of the central α-C atoms, C6 and C35, bonds tetrahedrally to a hydroxyl, two phenyls and a carboxylate with bond distances

[1] Supplementary data for this paper are available from the IUCr electronic archives (Reference: WS0002). Services for accessing these data are described at the back of the journal.

Table 2
Selected geometrical parameters (Å, °) for lithium benzilate hemihydrate.

Coordination around Li59	
Ow···Li59	2.01 (2)
O32···Li59	1.84 (2)
O30^{i}···Li59	1.98 (2)
O33···Li59	2.03 (2)
O33—Li59—Ow	111.4 (9)
O33—Li59—O30^{i}	109.8 (9)
O33—Li59—O32	82. 9 (8)
Ow—Li59—O30^{i}	108.9 (9)
O32—Li59—O30^{i}	128.4 (9)
Ow—Li59—O32	112.3 (9)
Coordination around Li60	
O3^{ii}···Li60	1.94 (2)
O1^{iii}···Li60	1.82 (2)
O32···Li60	1.97 (2)
O4^{iii}···Li60	2.03 (2)
O4^{iii}—Li60—O32	113.3 (9)
O1^{iii}—Li60—O3^{ii}	129.4 (9)
O1^{iii}—Li60—O32	111.6 (9)
O1^{iii}—Li60—O4^{iii}	83.9 (8)
O3^{ii}—Li60—O32	99.5 (8)
O3^{ii}—Li60—O4^{iii}	119.4 (9)
Ambient around the water molecule	
Ow···Li59	2.01 (2)
Ow···O1	2.59 (2)
Ow···Ow^{iii}	3.04 (2)
Ow···Ow^{ii}	3.04 (2)
Li59—Ow—O1	130.1 (9)
Li59—Ow—Ow^{iii}	94.7 (8)
Li59—Ow—Ow^{ii}	101.5 (9)
O1—Ow—Ow^{iii}	87.4 (8)
O1—Ow—Ow^{ii}	114.4 (9)
Ow^{iii}—Ow—Ow^{ii}	130.8 (9)
Other bond distances and torsion angles	
O1—C7	1.170 (3)
O3—C7	1.329 (5)
O30—C36	1.218 (5)
O32—C36	1.301 (5)
O4—C6—C8—C9	105.2 (2)
O4—C6—C8—C17	−70.4 (2)
O4—C6—C19—C20	160.1 (2)
O4—C6—C19—C28	−14.7 (2)
O33—C35—C48—C49	−15.1 (2)
O33—C35—C48—C57	157.2 (1)
O33—C35—C37—C46	−65.5 (2)
O33—C35—C37—C38	111.7 (1)

Symmetry codes: (i) $x, -1+y, z$; (ii) $\frac{3}{2}-x, -\frac{1}{2}+y, -z$; (iii) $\frac{3}{2}-x, \frac{1}{2}+y, -z$.

and angles shown in Table 2. The orientations of the phenyl rings in the benzilate moieties are those of propeller blades, as found in potassium benzilate (Vyas *et al.*, 1978), in a bis(benzilato)penta-coordinated silicate organometallic complex (Tacke *et al.*, 1994) and in the various benzilate derivatives of quaternary ammonium salts that encompass the anti-muscarinic drugs (Meyerhöffer & Carlström, 1969; Carpy *et al.*, 1979; Leger *et al.*, 1979; Sabatino *et al.*, 1994; Kiesewetter, Flippen-Anderson & Eckelman, 1995; Kiesewetter, Silverton & Eckelman, 1995). This conformation minimizes the repulsive interactions between the geminal phenyl rings. If the torsion angles C57—C48—C35—O33 (−157.1°) and C20—C19—C6—O4 (−160.3°) are taken as indicative of the conformation adopted by the phenyl rings, then these values are in agreement with those measured in eight benzilate fragments found in the Cambridge Structural Database (Allen & Kennard, 1993) [mean value: −166.0°; smallest value: −156.8°, largest value: −173.7°]. Furthermore, *ab initio* molecular orbital optimization of the benzilate ion geometry, which was carried out using the program *GAUSSIAN*94 (Frisch *et al.*, 1995) with a 6-31+G(d) basis set, yielded a value of −154.6° for the aforementioned torsion angle. From these calculations it was also inferred that small deviations from the rendered conformation (such as ±10° rotations about one of the phenyl rings) were tolerated before the hydrophobic repulsion between phenyl rings became significant.

Both Li atoms have a similar slightly distorted tetragonal pyramidal tetra-coordination stereochemistry, with Li—O distances between 1.844 and 2.029 Å for Li59 and 1.827 and 2.028 Å for Li60 (see Table 2). However, the coordination spheres are constructed somewhat differently: Li60 coordinates with one hydroxyl and three carboxylate O atoms from three different benzilate anions, whose carboxylate groups act as unidentate ligands, while Li59 coordinates to one hydroxyl and two O atoms also belonging to carboxylate groups from different benzilate anions, and completes its coordination number by linking to the oxygen of the nearby water molecule. The O32 acts as the bridging link between Li59 and Li60, which are separated by an Li—Li distance of 3.18 Å.

3.2. Close packing and hydrogen bonds

The geometries of the most relevant cohesive interactions that contribute to the packing of the lithium benzilate are depicted in Table 3. The structure in the solid state (see Fig. 3) is a coordination polymer based on dimeric units with the formula $[Li_2(C_{14}H_{13}O_3)_2\cdot H_2O]$ interacting strongly by coordination metal–oxygen interactions and O—H···O hydrogen bonds with other dimeric units related by the symmetry operation $\frac{3}{2}+x, \frac{1}{2}+y, -z$. These tetramers build up square helical one-dimensional channels running parallel to the [010] direction. The negatively charged benzilates are arranged in such a way that carboxylate and hydroxyl groups point towards the center of the channels, while the bulkier hydrophobic phenyl groups protrude forming the outer region. Lithium ions locate at bonding distances from the oxygen-rich inner region to compensate for the negative charge of the benzilate frame. Water molecules, sitting very near the center of the channels where the 2_1 axes are located, interact by hydrogen bonds Ow—H2w···Ow forming infinite chains that run parallel to the [010] direction (Fig. 3). In addition, the water molecule interacts with both benzilate ions through Ow—H1w···O1 and Ow—H1w···O32 (at $\frac{3}{2}-x, -\frac{1}{2}+y, -z$) *via* bifurcated donor hydrogen bonds (Desiraju & Steiner, 1999). These hydrogen bonds, together with the coordination sphere based on Li—O interactions constructed around both Li^+ ions, make up the aggregate interactions that hold together the inner portions of the one-dimensional channels.

The outer regions of the channels are abundant in phenyl rings and, hence, aromatic $\pi\cdots\pi$ stacking interactions are

Table 3
Hydrogen bonds for lithium benzilate hemihydrate.

γ is defined as the angle between the X—H vector and the normal to the plane of the phenyl ring. The centers of gravity of the phenyls are:

	x	y	z
Ph1	0.5974(2)	0.64112(8)	0.19521(2).
Ph2	0.91281(1)	0.83102(8)	0.47307(4)

D—H···A	D—H (Å)	H···A (Å)	D···A (Å)	D—H···A (°)
Shortest hydrogen bonds inside the channels				
Ow—H1w···O1	1.00 (2)	1.77 (2)	2.607 (3)	138 (3)
Ow—H1w···O32^{i}	1.00 (2)	2.54 (3)	3.252 (5)	128 (2)
Ow—H2w···Ow^{i}	1.001 (3)	2.242 (7)	3.050 (4)	136.8 (2)

	H···Ph (Å)	γ (°)	X—H···Ph (°)	X···Ph (Å)
Shortest X—H···ring (π) interactions outside the channels				
C11—H12···Ph1^{ii}	2.848 (2)	10.51	160.3 (2)	3.804 (1)
C15—H16···Ph2 ^{iii}	3.134 (2)	1.85	164.8 (3)	4.108 (1)
C24—H25···Ph2 ^{iv}	2.891 (3)	14.21	149.6 (4)	3.788 (1)

Symmetry codes: (i) $\frac{3}{2}-x,-\frac{1}{2}+y,-z$; (ii) $1-x,2-y,-z$; (iii) $\frac{3}{2}-x,\frac{1}{2}+y,-z$; (iv) $\frac{3}{2}-x,-\frac{1}{2}+y,1-z$.

expected to be present. These interactions exist but they are very weak because distances greater than 5.10 Å separate adjacent phenyl rings that have the appropriate orientation for the overlap of the π orbitals. However, there are three intermolecular C—H···Ph hydrogen bonds (Braga, Grepioni & Tedesco, 1998) that contribute to the supramolecular aggregation of the structure in the form of infinite chains constructed with C24—H24···Ph2 and C15—16···Ph2 interactions running parallel to the [001] direction, and infinite zigzag chains of C11—H12···Ph1 interactions running parallel to the [100] direction (Fig. 4).

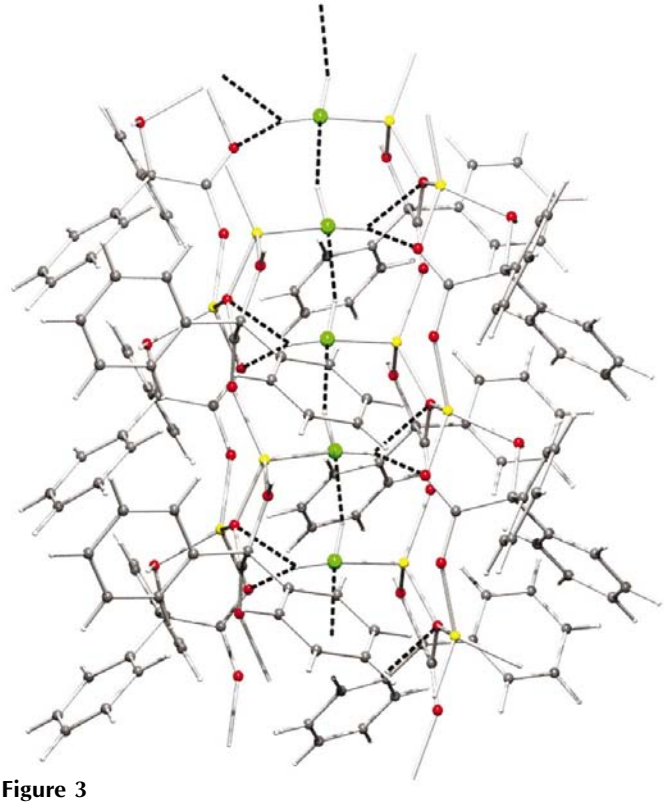

Figure 3
The water molecule acts as the cohesive entity inside the channels. The view shows the infinite chain of water molecules linked by hydrogen bonds and the bifurcated donor hydrogen bond form with carboxylate O atoms from the two nearest benzilate anions.

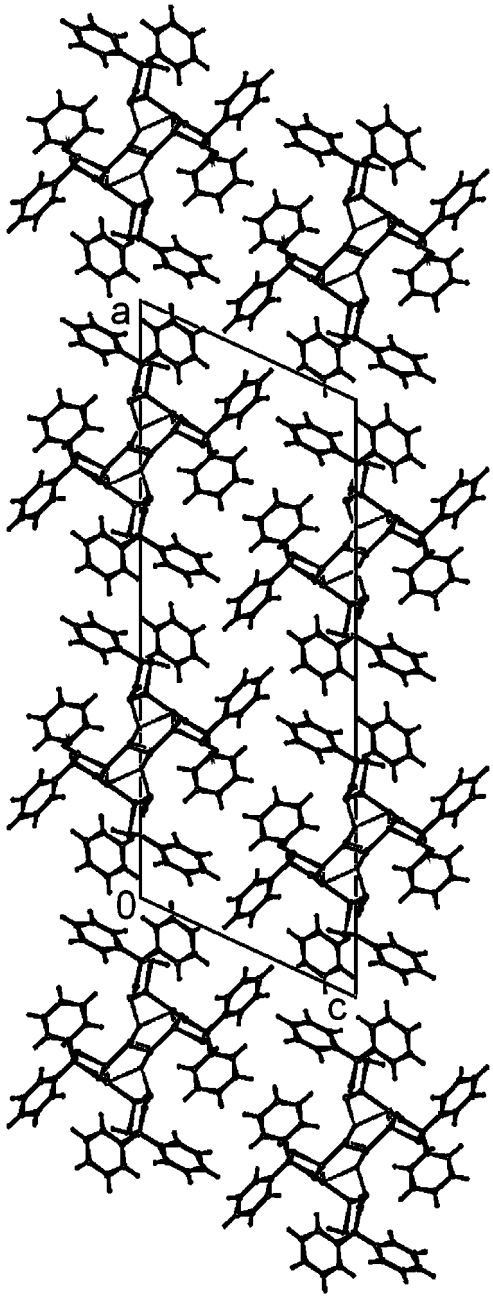

Figure 4
View of the lithium benzilate hemihydrate structure down the b axis showing the orientation of the phenyl rings in the outer region of the channels that propagate C—H···Ph interactions.

4. Conclusions

From synchrotron powder diffraction data, the molecular and crystal structure of lithium benzilate hemihydrate have been determined. This work was achieved by the combination of the recently developed direct-space search method based on a simulated-annealing global minimization (Newsam *et al.*, 1992; Harris *et al.*, 1994; Andreev *et al.*, 1996; David *et al.*, 1998), and the long-established difference Fourier maps that were helpful in completing the structure. The final solution required the localization of 37 non-H atoms in the asymmetric unit. The balance between the two prominent characteristics of the propeller-shaped benzilate anions marks the assembly of the molecules in the solid state: the hydrophobicity of the bulky phenyl rings and the localized hydrophilicity of the carboxylate and hydroxyl groups. In turn, a structure results consisting of one-dimensional helical fourfold channels parallel to [010], which resemble those of zeolites. Hydrophobic phenyl rings poke out of the channels, while hydrophilic groups line the interior. The resemblance with zeolitic structures goes even further and the interior of the channels can be perceived as being populated with lithium ions, interacting actively with occluded water molecules, and carboxylate and hydroxyl groups of the benzilate anions. Hydrogen bonds of various strength acting in the interior and exterior of the channels contribute to the supramolecular aggregation of the structure. This diversity of intermolecular forces was anticipated (Braga, Grepioni & Desiraju, 1998); this being the hallmark of many alkali and metal complexes that manifest hydrogen bonding and coordination polymer formation.

It is worth emphasizing that essential to the structure solution and the degree of structural detail attainable in this work was the preparation of a crystalline sample that produced a sharp diffraction pattern, and the high instrumental resolution and count rate offered by BM16 at the ESRF.

We thank the ESRF for provision of beam time in the BM16 powder diffraction beamline. AJM wishes to thank the ESRF, FONACIT and Universidad de Los Andes in Mérida, Venezuela, for providing support during the sabbatical spent at the ERSF.

References

Allen, F. H. & Kennard, O. (1993). *Chem. Des. Autom. News*, **8**, 31–37.
Andreev, Y. G., Lightfoot, P. & Bruce, P. G. (1996). *J. Chem. Soc. Chem. Commun.* pp. 2169–2170.
Boultif, A. & Louër, D. (1991). *J. Appl. Cryst.* **26**, 128–129.
Braga, D., Grepioni, F. & Tedesco, E. (1998). *Organometallics*, **17**, 2669–2672.
Braga, D., Grepioni, F. & Desiraju, G. R. (1998). *Chem. Rev.* **98**, 1375–1405.
Carpy, H., Leger, J. M. & Gadret, M. (1979). *Acta Cryst.* B**35**, 882–886.
David, W. I. F., Shankland, K., Cole, J., Maginn, S., Motherwell, W. D. H. & Taylor, R. (2001). *DASH User Manual.* Cambridge Crystallographic Data Centre, Cambridge, UK.
David, W. I. F., Shankland, K. & Shankland, N. (1998). *J. Chem. Soc. Chem. Commun.* pp. 931–932.
Desiraju, G. R. & Steiner, T. (1999). *The Weak Hydrogen Bond in Structural Chemistry and Biology*. IUCr Monographs on Crystallography 9. Oxford University Press.
Drescher, D. G., Kerr, T. P. & Drescher, M. J. (1999). *Brain Res.* **845**, 199–207.
Finger, L. W., Cox, D. E. & Jephcoat, A. P. (1994). *J. Appl. Cryst.* **27**, 892–900.
Fitch, A. N. (1995). *Nucl. Instrum. Methods Phys. Res. B*, **97**, 63–69.
Frisch, M. J., Trucks, G. W., Schlegel, H. B., Gill, P. M. W., Johnson, B. G., Robb, M. A., Cheeseman, J. R., Keith, T., Petersson, G. A., Montgomery, J. A., Raghavachari, K., Al-Laham, M. A., Zakrewski, V. G., Ortiz, J. V., Foresman, J. B., Cioslowski, J., Stefanov, B. B., Nanayakkara, A., Challacombe, M., Peng, C. Y., Ayala, P. Y., Chen, W., Wong, M. W., Andres, J. L., Replogle, E. S., Gomperts, R., Martin, R. L., Fox, D. J., Binkley, J. S., Defrees, D. J., Baker, J., Stewart, J. P., Head-Gordon, M., Gonzales, C. & Pople, J. A. (1995). *Gaussian.* Pittsburgh PA, USA.
Harris, K. M., Tremayne, M., Lightfoot, P. & Bruce, P. G. (1994). *J. Am. Chem. Soc.* **116**, 3543–3547.
Hiramatsu, Y., Eckelman, W. C. & Baum, B. J. (1994). *Life Sci.* **54**, 1777–1783.
Johnston, M. V., Reindel, F. O., Silverstein, F. S., Young, A. B. & Penney, J. B. (1985). *Dev. Brain Res.* **19**, 195–203.
Kiesewetter, D. O., Flippen-Anderson, J. L. & Eckelman, W. C. (1995). *J. Labelled Comput. Radiopharm.* **37**, 686–698.
Kiesewetter, D. O., Silverton, J. V. & Eckelman, W. C. (1995). *J. Med. Chem.* **38**, 1711–1719.
Laar, B. van & Yelon, W. B. (1984). *J. Appl. Cryst.* **17**, 47–54.
Larson, A. C. & Von Dreele, R. B. (1998). *GSAS.* Los Alamos National Laboratory, Los Alamos, NM, USA.
Lee, K. S., Frey, K. A., Koeppe, R. A., Buck, A., Mulholland, G. K. & Kuhl, D. E. (1996). *J. Cereb. Blood Flow Metab.* **16**, 303–310.
Leger, J. M., Gadret, M. & Carpy, A. (1979). *Acta Cryst.* B**35**, 886–890.
Meyerhöffer, A. & Carlström, D. (1969). *Acta Cryst.* B**25**, 1119–1126.
Molecular Simulations Inc. (2001). *Material Studio*, Version 1.2. San Diego, CA, USA.
Mora, A. J., Delgado, G., Fitch, A. N., Wright, J., Brunelli, M., Ramírez, B. & Díaz de Delgado, G. E. (2003). In preparation.
Newsam, J. M., Deem, M. W. & Freeman, C. M. (1992). *Accuracy in Powder Diffraction*, edited by E. Prince & J. K. Stalick, Vol. II. *NIST* Spec. Publ. No. 846, pp. 80–91.
Pawley, G. S. (1981). *J. Appl. Cryst.* **14**, 357–361.
Rojas, L. (2001). Tesis de Licenciatura, Universidad de Los Andes, Mérida, Venezuela.
Rietveld, H. M. (1969). *J. Appl. Cryst.* **2**, 65–71.
Sabatino, P., Recanatini, M., Tumiatti, V. & Melchiorre, C. (1994). *Acta Cryst.* C**50**, 640–645.
Smith, G. S. & Snyder, R. L. (1979). *J. Appl. Cryst.* **12**, 60–65.
Tacke, R., Lopez-Mias, A. & Jones, P. G. (1994). *Organometallics*, **13**, 1617–1623.
Vyas, M., Sakore, T. D. & Biswas, A. B. (1978). *Acta Cryst.* B**34**, 1345–1347.
Wilson, A. J. C. (1995). Editor. *International Tables for Crystallography*, Vol. C. Dordrecht: Kluwer Academic Publishers.
Wolff, P. M. de (1968). *J. Appl. Cryst.* **1**, 108–113.